Case Studies in Nondestructive Testing and Evaluation 6 (2016) 17–25

Contents lists available at ScienceDirect

Case Studies in Nondestructive Testing and Evaluation

www.elsevier.com/locate/csndt

Comparison of medical and industrial X-ray computed tomography for non-destructive testing

Anton du Plessis [a,b,*], Stephan Gerhard le Roux [a], Anina Guelpa [a]

[a] CT Scanner Facility, Central Analytical Facilities, Stellenbosch University, Stellenbosch, South Africa
[b] Physics Department, Stellenbosch University, Stellenbosch, South Africa

ARTICLE INFO

Article history:
Available online 1 August 2016

ABSTRACT

Industrial X-ray computed tomography (CT) is an emerging laboratory-based non-destructive testing technique used in a variety of applications for samples ranging from 1 mm to usually 300 mm in diameter. Usually, microCT scanners are used for industrial non-destructive testing due to the superior resolution possible compared to medical CT scanners, but it is not generally known that medical CT scanners can produce reasonable results when high resolution is not needed. As demonstrated in this case study of very dense objects, far shorter scan time is required, compared to conventional laboratory industrial CT systems, consequently being a better solution for applications such as quick scout-scans, high throughput applications and larger objects. This case study makes use of four typical industrial test objects, specifically chosen as candidates which would be expected to be too dense for relatively low-voltage medical scanners. The respective test objects were scanned with both medical and microCT scanners and the results compared for the purpose of industrial non-destructive analysis. The test objects are a steel turbine blade, a titanium casting, a concrete cylinder with aggregate stones and porosity, and a concrete block with metal fiber reinforcement.

1. Introduction

X-ray Computed Tomography (CT) provides a significant improvement in its ability to detect small defects, compared to traditional radiography, hence its growing use in industrial applications [1]. Its use is also widely found in academic research, with recent reviews in food sciences [2], material sciences [3] and geosciences [4]. The use of X-ray CT in the field of metrology and even inline applications using fast scanning industrial CT systems is also rapidly growing, see e.g. [5–7].

Medical CT and industrial CT are based on the same underlying physics principles [8] but differ in system layout and design, due to their different application types. Medical CT has been well described in [9] and compared to industrial CT, it seems in principle not suitable for large dense objects such as steel parts or concrete blocks, due to the limit of 120–130 kV for most such systems. Since higher X-ray voltages are possible with industrial CT systems which allow higher penetrating power, industrial CT or microCT should be improved compared to medical CT scans with respect to image quality for dense objects, due to the improved penetrating power [5]. Industrial CT scanners are usually used for quantitative dimensional analysis [10] while medical CT scanners are optimized for qualitative viewing (image quality of human subjects) and specifically optimized for low dose, while dimensional accuracy is not crucial for medical diagnosis.

* Corresponding author.
E-mail address: anton2@sun.ac.za (A. du Plessis).

http://dx.doi.org/10.1016/j.csndt.2016.07.001

Medical CT has over the years been used for industrial applications, especially before present-day microCT capabilities were available commercially. Especially in the fields of aerospace composites (carbon and glass fiber composite materials) the method has been used widely, see e.g. [11].

However, despite the obvious accuracy and quality advantages of industrial CT systems, the cost of such systems mostly exceed that of medical CT. Industrial CT systems range in price for a basic system capable of 225 kV with micro focus CT capability from 300 000 up to more than 1 000 000 Euros. While lower-cost systems down to 60 000 Euros are available, they are not capable of such high voltages and have other sample size limitations (i.e. Benchtop systems only suitable for small samples). The costs above are also mentioned in a recent perspective on industrial CT [12]. Medical CT systems range in price from 60 000 up to 300 000 Euros for the latest models [13], making them more affordable. Besides purchase price, the scan-time strongly affects the price per scan to the end-user. Typical industrial CT scan times are still 30–60 minutes or more depending on the quality required (see e.g. [14]) while medical CT scanners complete a full scan in 5 seconds (plus a few minutes cool-down time for the system). This difference is significant and allows, e.g., at least 10 samples to be scanned in a medical CT system in the same time as one is scanned in an industrial CT system (with very conservative estimates). Of course, faster industrial scanners are available and in use today dedicated for industrial CT and which are meant for in-line process applications, but these systems are even more costly than the 1 000 000 Euro price mentioned above. The high-throughput and low cost of medical CT is therefore of interest and its use as an alternative or complementary tool is worthy of investigation for some applications.

In this work we test the exact same four large objects on medical and industrial microCT scanners and describe the differences and respective advantages and disadvantages of the two techniques for these type of objects. The choice of objects was made such that these are challenging even for industrial CT with 225 kV micro focus capability, and which are expected to be too dense for low-voltage medical CT. Obviously lower density objects such as glass fiber or carbon fiber composites, wood products, polymers or even lighter metal alloys would result in much improved quality from the medical scans. This is the first direct quantitative comparison between industrial CT and medical CT reported in the scientific literature.

2. Method

Medical CT scans were conducted at Stellenbosch Mediclinic Hospital, with support from Drs Van Wageningen and Partners. The system used was a Siemens Somatom with 130 kV and 250 mA, with scan times usually 5–10 seconds per object, though the system needs cooling down between scans of a few minutes. Voxel resolution for the medical CT scans was fixed at 700 μm. The medical scans were done with standard pre-loaded settings. MicroCT scans were done at the Stellenbosch University CT Facility [15]. The system used was a General Electric V|Tome|X L240, using 220 kV and 180–200 μA, with scan times 1–2 hours for each object. All objects were scanned with 3000 projection images in total, with no averaging or skipping of images. Detector shift was activated to minimize ring artifacts from the center of rotation and the camera gain was set to maximum, while beam filtration was 1.5 mm copper. The voxel resolution of the microCT scans varied from 80–160 μm depending on the object size: steel turbine blade 100 μm; titanium casting 86 μm; concrete cylinder with porosity 80 μm; concrete block with metal fibers 121 μm. Reconstruction was done with beam hardening correction values of 8 or 8.5.

Data was visualized and analyzed using VGStudioMax 2.2 and 3.0 including additional modules for defect detection, orientation analysis and CAD comparison analysis. In the case of the microCT data, a single data filtering was applied to reduce noise and simplify the segmentation process, in the form of an adaptive Gaussian filter. Segmentation was done using a combination of region growing tools and the advanced surface determination function, making use of the selected region as a starting contour for the surface determination. A similar process was applied to the medical CT data. Data set sizes of the medical CT scans in DICOM format totaled 200 MB while the corresponding slice image stack from the microCT scan was approximately 3 GB, excluding raw data which totaled 20 GB.

The four large objects under investigation in this case study are shown in Fig. 1. These are a concrete block with metal fiber reinforcement, a steel turbine blade, a concrete cylinder and a titanium casting that has been subjected to hot isostatic pressing (HIPping).

The concrete with metal fibers is of interest for civil engineering applications and is being researched by a local research group for strengthening of concretes [16]. The steel turbine blade was provided as a test sample from an industrial client: the non-destructive testing of these blades is an ongoing interest in industrial applications due to premature failures causing significant and costly damage and downtime in power plants. In one approach to improve image quality of edge data from such samples, a data fusion approach between microCT data and ultrasonic testing was applied, e.g. [17]. The concrete cylinder sample is similar to, but larger than, that used in a recent multiscale porosity analysis study [18]. The titanium casting was studied before HIPping and reported in a case study previously [11]. The same titanium investment casting process from which this part was made, was also studied before and after HIPping using test rods, therefore not actual complex parts as shown here [19] and is an ongoing research and development effort.

Fig. 1. Photo of the samples with a 30 cm scale bar at the bottom – on the left is a concrete block with metal fiber reinforcement, in the middle is a steel turbine blade, on the top right is a concrete cylinder and on the bottom right is a titanium investment casting.

3. Results and discussions

3.1. Steel turbine blade

The steel turbine blade is a classic industrial part where the interest can be to investigate its interior or exterior for possible cracks and defects, or where an accurate surface model data set is required. Its dimensions are 175 mm long, approximately 29 mm wide at the blade and approximately 10 mm on the blade's thickest section (in the middle). This blade has no internal cooling channels. Due to the density, high X-ray power is required which can limit the resolution of the scan data, thereby limiting the ability to detect cracks or small porosity. The example presented does not show any detectable cracks at the scan resolution of 100 μm but it makes a good example for checking changes relative to its original shape (e.g. indicating wear locations). Fig. 2 shows CT views of the medical CT and the microCT data and the two overlaid virtually. Clearly the microCT data is smaller, and some image artifacts are present in the medical CT data such as ring artifacts and lack of contrast. Using the same image analysis methods in the same software, surface determinations are done using a global thresholding combined with local refinement. The surface data can be exported as STL files or used for comparing the two scans as is done in Figs. 2(a) and (b) using a computer-aided drawing (CAD) comparison. The warmer colours (orange, red) show where the largest positive deviation is found, which in this case indicates where the medical CT data deviates more from the microCT data. The process is based on a best-fit alignment of the two data sets. The largest deviation is found on the inside of the hollow of the blade: the reason for this deviation is due to an image artifact which can be partly due to lack of good penetration by the medical CT but also may be exaggerated in this geometry by the relatively poorer resolution. The quantitative statistical variance is shown in Fig. 2(c) where the peak around 2.2 mm corresponds to this hollow region. The bulk of the data is slightly larger than the microCT data set, which can be explained by the low voltage which causes a lack of contrast in the medical CT data. This results in the edge of the object measuring slightly larger than it really is, for this type of object.

The artifacts in the medical scan result in differences compared with the microCT data set, as observed most in the region on the inside of the blade curvature. However, the medical CT data is reasonably good when considering it was recorded in a few seconds and is in most places less than 1 mm offset. Therefore it can be concluded that medical CT can be more suitable for high throughput reverse engineering applications where dimensional accuracy is not required, i.e. when only macro changes are required to be observed.

3.2. Titanium investment casting

A titanium investment casting which had been subjected to hot isostatic pressing (HIPping) was scanned by both medical CT and microCT. In this sample the HIP treatment was expected to close the porosity. In the process of closing the porosity, some large internal pores cause the surface to become indented, at the location of the pore. The interest in this example is therefore to visualize and detect surface defects, but also inspect the interior for any remaining pores, none of which were found in this example at the scan resolution of 86 μm. Figs. 3(a) and (b) show three-dimensional (3D) views of the scans

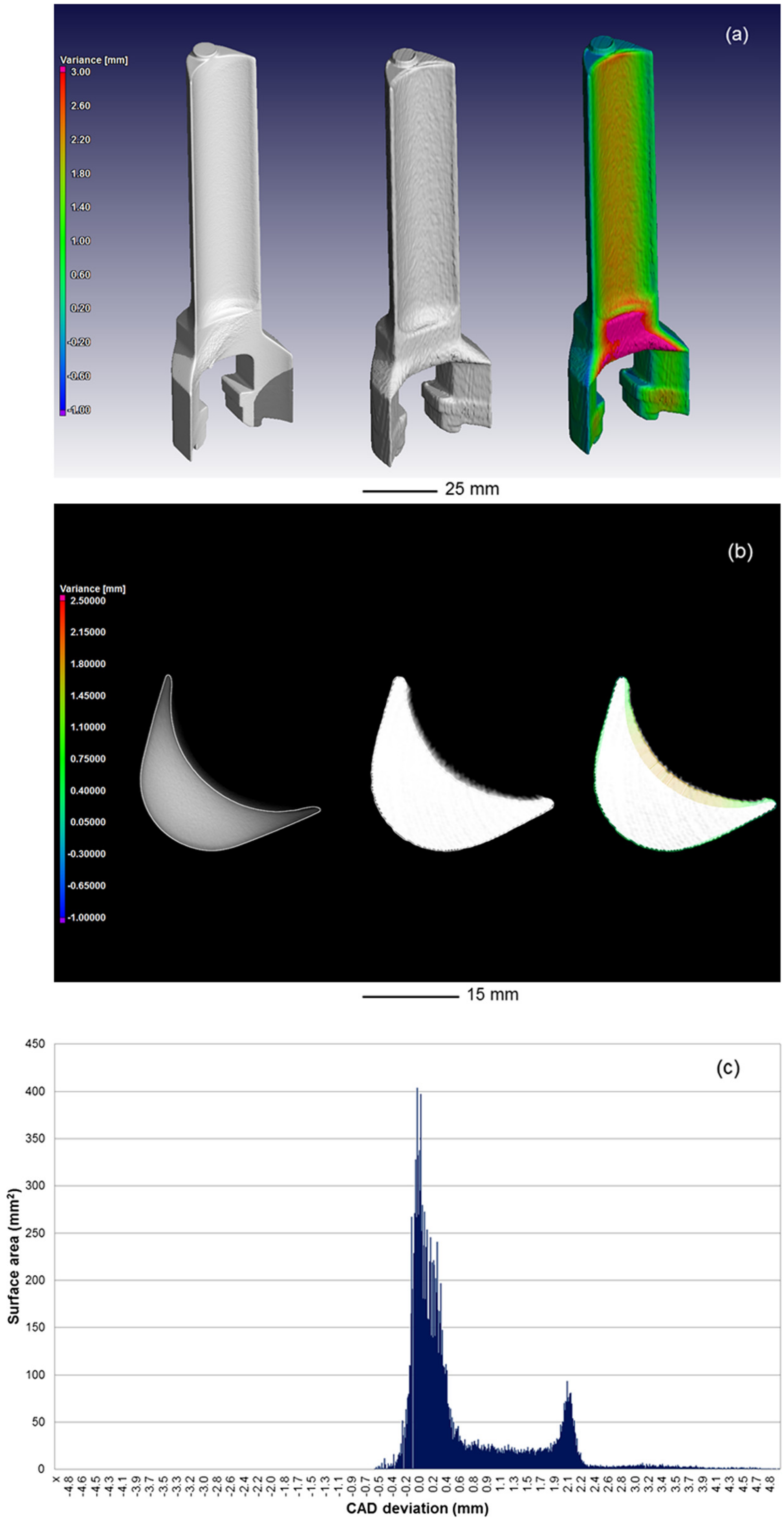

Fig. 2. Steel turbine blade comparison between medical and industrial microCT (from left to right) microCT, medical CT and CAD comparison (overlay): (a) 3D view, (b) slice view, (c) statistical deviation data. The warm colours indicate where the medical CT data deviates the most from the microCT data.

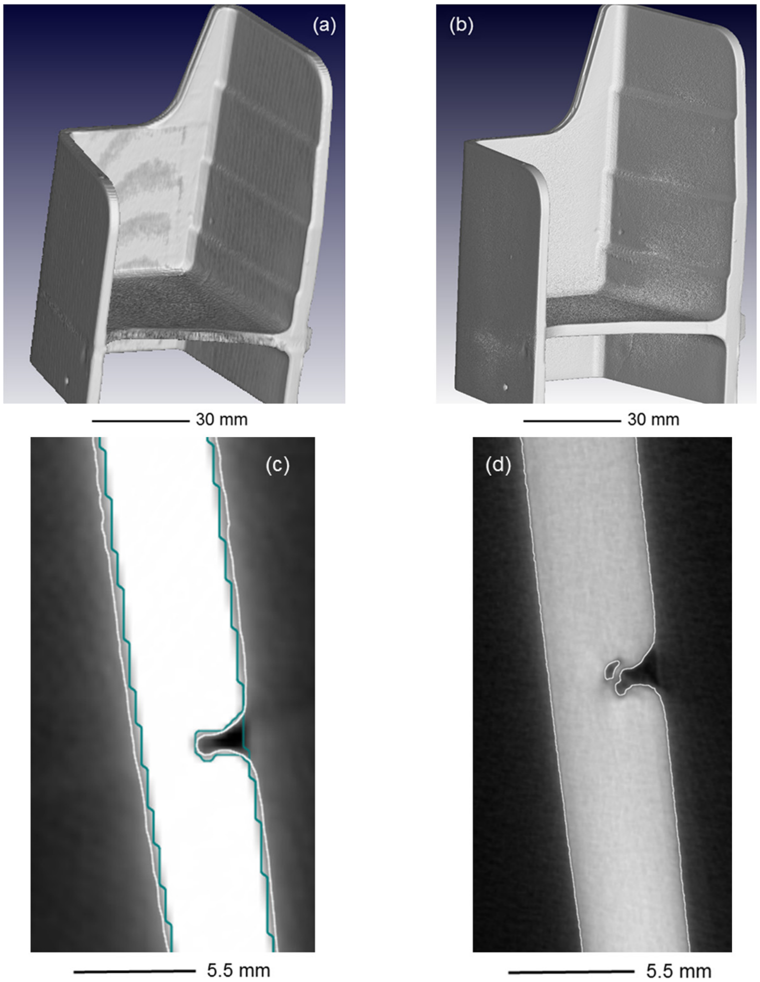

Fig. 3. Titanium investment casting 3D view with surface defects, comparison of medical CT (left) and microCT (right) shown here in (a) 3D views and (b) slice views.

with medical CT to the left and microCT to the right. Both are good representations of the sample, with the medical CT having some lack of penetration causing slight inaccuracy on the horizontal flat section in the middle (darker colour in 3D view). All surface features are visible in both scans, including indentation caused by porosity shown in Figs. 3(c) and (d) in slice images. Clearly the medical scan lacks some resolution and clarity but the feature is clearly visible and can be well discriminated.

The ability of medical CT to detect surface defects is thus considered sufficient, for large enough features. The feature of interest here is 2 mm wide and 2.5 mm deep. Some additional small features are observed in the microCT which are missed in the medical CT data, these include a number of inclusions of approximately 400 µm in diameter, and some small surface indentations of 200 µm (not shown here). Considering the speed of data acquisition, the conclusion is that medical CT would be the preferred choice for routine non-destructive testing for surface defects, as well as large internal defects in such parts. However, for defects below 700 µm, the improved resolution of microCT would be the preferred choice.

3.3. Large concrete cylinder

A large concrete cylinder (96 mm high and 68 mm diameter) was scanned on both medical and microCT scanners. This sample contains aggregate stones, concrete and porosity of a large range of sizes, making it a good quality indicator for X-ray CT scans, especially for quantitative defect analysis. Both medical and microCT slice images from the side view and top views are shown in Fig. 4 side by side (they are aligned to show the same features). All features are visible in both data sets, including the porosity as black spots, the edges of the sample are clear and the aggregate stones are also visible in both. It is also clear that the resolution of the microCT data is better, as it was set to 0.1 mm vs the medical scan of 0.7 mm. A defect analysis was done on both data sets and results are shown in 3D in Fig. 5. In this image, the warmer colours indicate larger-diameter voids while the cooler blue colours indicate smaller diameter pores. Clearly the medical CT data overestimates the pore sizes, possibly due to the weaker resolution. In the medical scan, the smallest pores detected

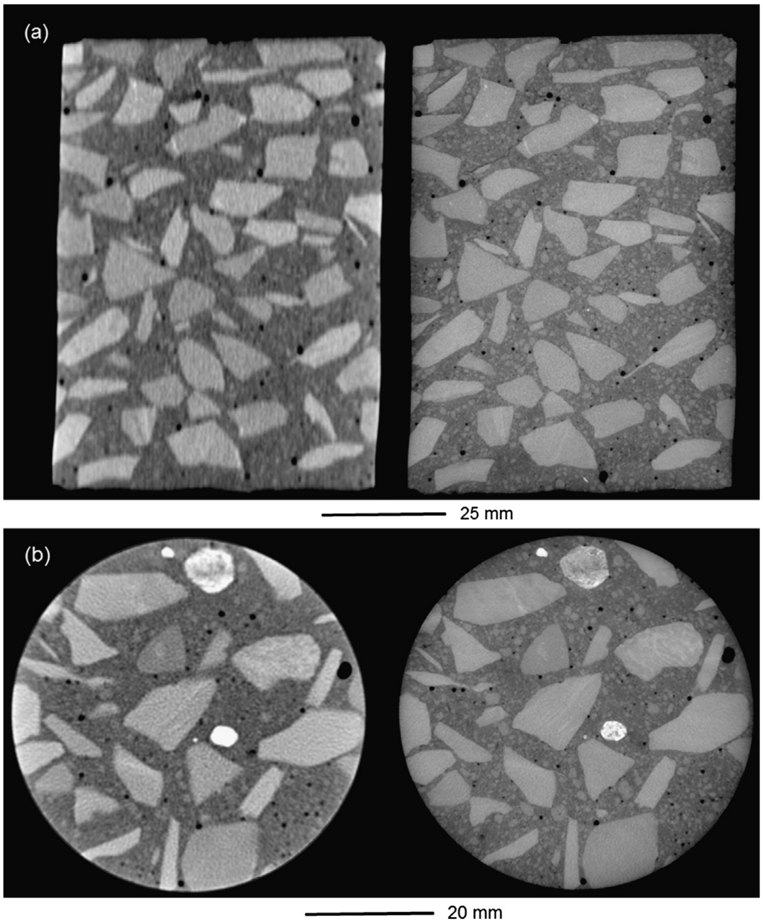

Fig. 4. Concrete cylinder medical CT (left) and microCT (right) slice images from (a) side and (b) top views.

are 0.8 mm diameter while in the microCT the smallest pores detected are 0.2 mm. In total the medical CT detects 1916 pores while the microCT detects significantly more: 11603, mainly due to the large numbers of small pores present in the sample below 800 μm. The statistical pore size histogram is shown in Fig. 5(b) indicating the size ranges of the majority of pores in the two scans.

From these results it can be concluded that for porosity measurement using medical CT scans, large pores are positively identified but there is a significant overestimate of the pore sizes, with the 3D views showing some slight form of elongation most likely due to voxels that are not isotropic (not of same size). Considering the goal of analysis, both medical CT and microCT might have applications in such samples. This might indicate that microCT is superior for defect analysis in general, as the dimensions of the defects are of significant importance in making decisions with regards to non-destructive analysis.

3.4. Large concrete block with metal fiber reinforcement

The final example is a large concrete block of dimensions $190 \times 150 \times 70$ mm^3 containing metal fiber reinforcement. Due to the sample size and X-ray penetration limitations, only one part of the block could be scanned on microCT and the scan time was almost 3 hours, compared to the medical scan of only a few seconds. It would be possible to take multiple microCT scans and stitch them together but this is extremely time consuming and data intensive. In both cases a 3D orientation analysis was done on the metal fibers as shown in Fig. 6, with red being vertical and blue horizontal.

Clearly the medical CT could scan the entire sample and produced good directionality information on the fibers. Upon closer inspection, the fibers are estimated larger than in the microCT data set which is not shown here. Clearly in this case a medical CT scan would be preferred especially for large numbers of samples, while dimensionally more accurate analysis could be done by microCT, possibly on smaller sections.

4. Conclusions

This case study indicates that medical CT scans can produce useful data in significantly reduced times, making it a definite good option for non-destructive testing, especially for large numbers of samples and where only moderate resolution

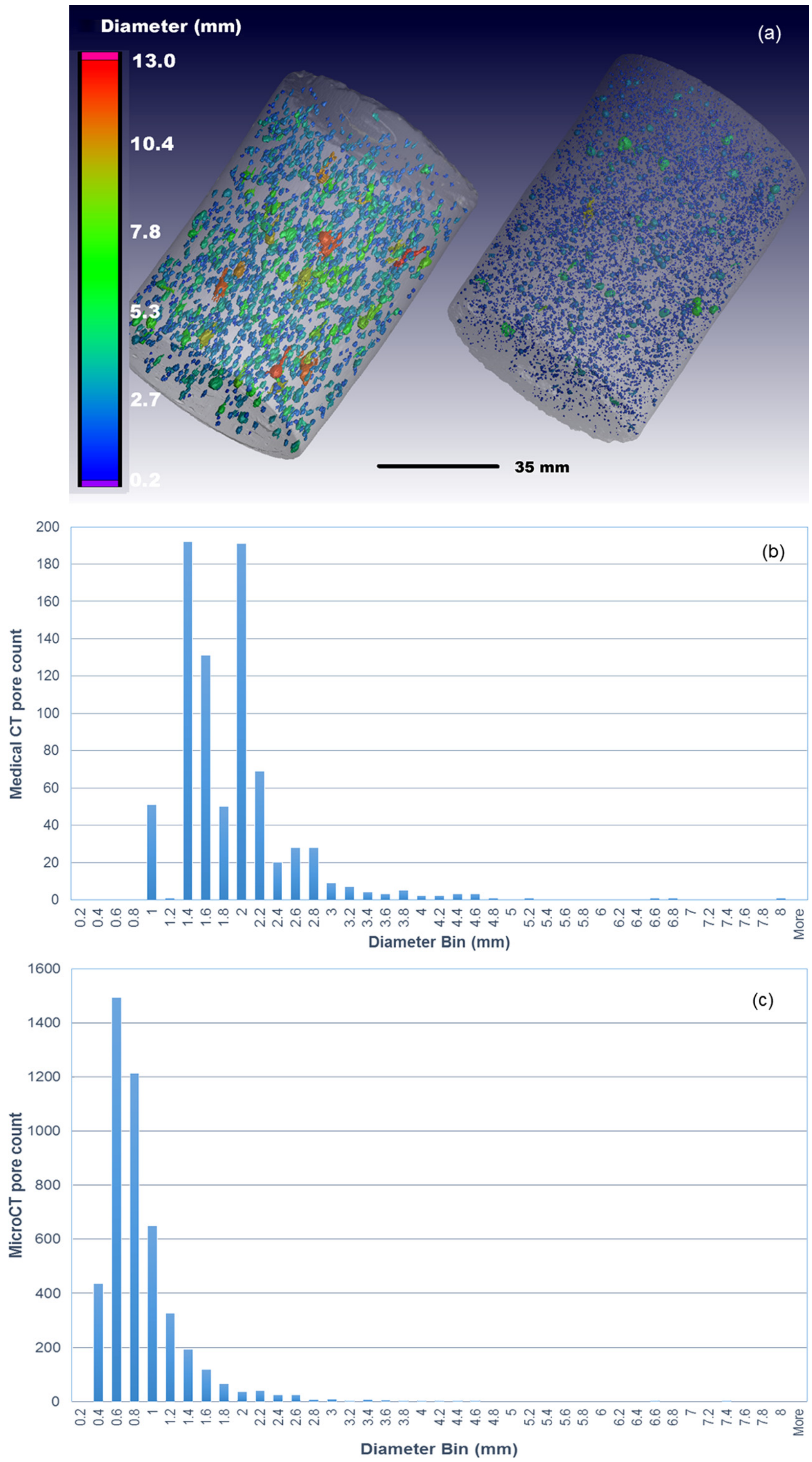

Fig. 5. Porosity analysis of a concrete cylinder from Medical CT and microCT showing (a) 3D colour coded pore size analysis (medical CT left and microCT right) and pore size distribution histograms: (b) medical CT, (c) microCT.

is required. Another advantage is its ability to scan larger objects than typical microCT systems (e.g. an entire concrete block could not be scanned in one scan volume on a microCT, but could have been done by 3-part scanning tripling the scan time in this case up to more than 4 hours). Data set sizes are significantly reduced, making its analysis and quick assessment

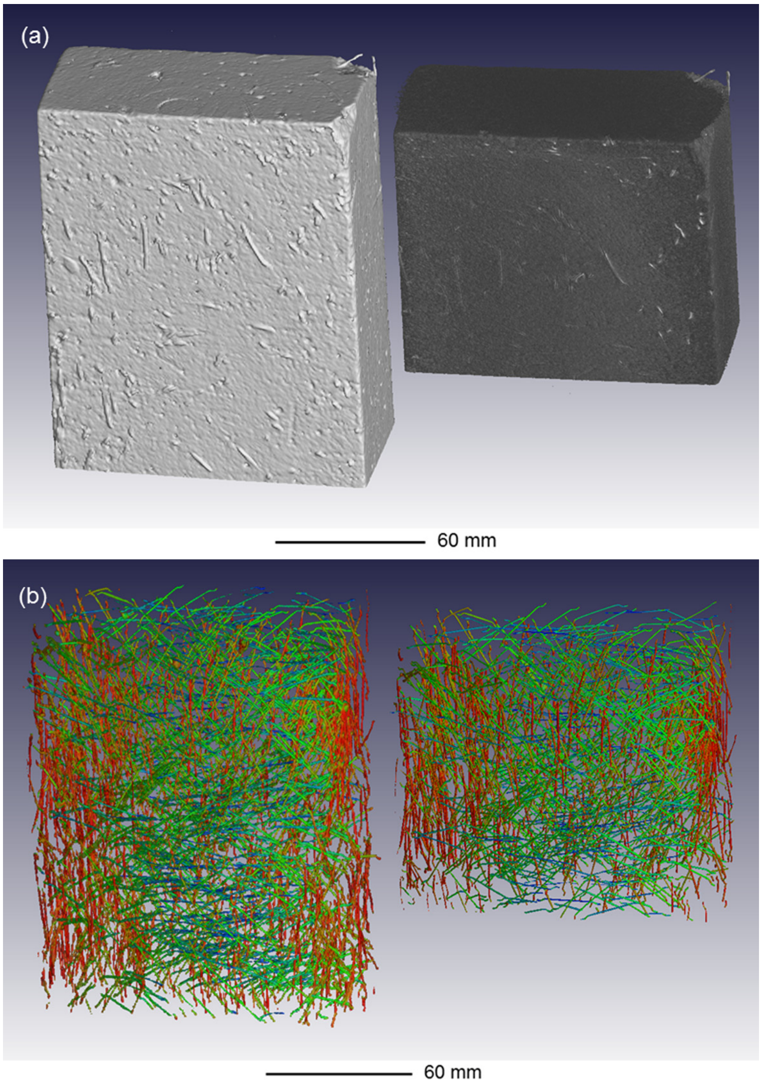

Fig. 6. Concrete block with steel fiber reinforcement analyzed by medical CT (left) and microCT (right), showing (a) a 3D surface view and (b) a transparent view with metal fibers colour-coded 3D angular orientation.

faster with reduced computational power necessary. However, industrial non-destructive analysis is usually not available at medical CT facilities, therefore analysis should still be done at industrial CT facilities or with industrial CT software.

The chosen test objects where specifically selected as challenging objects for microCT, i.e. they are all on the extreme limit of sample size and density possible for laboratory microCT (up to 225 kV), and therefore smaller or less dense objects will result in improved quality with respect to medical CT scans. However, larger objects will be impossible to scan with typical laboratory microCT, while medical CT could produce reasonable results, especially when only moderate resolution is required. Considering the artifacts, medical CT is however not good enough for industrial testing in general, but can find application in niche areas and for high throughput applications where critical components are tested which would not have been otherwise tested due to the time and cost constraints of typical microCT. It is envisaged that industrial non-destructive testing facilities could make use of both methods.

Acknowledgements

The medical CT scans were done at Stellenbosch Mediclinic Hospital (Drs Van Wageningen and Partners), we are thankful for their support of this project.

References

[1] De Chiffre L, Carmignato S, Kruth R, Schmitt JP, Weckenmann A. Industrial applications of computed tomography. Manuf Technol 2014;63(2):655–77.

[2] Schoeman L, Williams P, Du Plessis A, Manley M. X-ray micro-computed tomography (μCT) for non-destructive characterisation of food microstructure. Trends Food Sci Technol 2016;47:10–24.
[3] Maire E, Withers PJ. Quantitative X-ray tomography. Int Mater Rev 2014;59(1):1–43.
[4] Cnudde V, Boone MN. High-resolution X-ray computed tomography in geosciences: a review of the current technology and applications. Earth-Sci Rev 2013;123:1–17.
[5] Kruth JP, Bartscher M, Carmignato S, Schmitt R, De Chiffre L, Weckenmann A. Computed tomography for dimensional metrology. Manuf Technol 2011;60(2):821–42.
[6] Warnett JM, Titarenko V, Kiraci E, Attridge A, Lionheart WRB, Withers PJ, et al. Towards in-process x-ray CT for dimensional metrology. Meas Sci Technol 2016;27(3):35401–15.
[7] Léonard F, Brown SB, Withers PJ, Mummery PM, McCarthy MB. A new method of performance verification for x-ray computed tomography measurements. Meas Sci Technol 2014;25(6):65401–11.
[8] Kak AC, Slaney M. Principles of computerized tomographic imaging. Society for Industrial and Applied Mathematics; 2001.
[9] Kalender WA. Computed tomography: fundamentals, system technology, image quality, applications. John Wiley & Sons; 2011.
[10] Bartscher M, Hilpert U, Goebbels J, Weidemann G. Enhancement and proof of accuracy of industrial computed tomography (CT) measurements. Manuf Technol 2007;56(1):495–8.
[11] Bossi RH, Georgeson GE. Composite structure development decisions using X-ray CT measurements. Mater Eval 1995;53(10).
[12] Kastner J. Preface: Special issue on the 6th conference on industrial computed tomography 2016 (iCT2016). Case Stud Nondestruct Test Eval 2016.
[13] http://info.blockimaging.com/how-much-does-a-ct-scanner-cost/, accessed 14.06.16.
[14] Du Plessis A, Rossouw P. X-ray computed tomography of a titanium aerospace investment casting. Case Stud Nondestruct Test Eval 2015;3:21–6.
[15] http://www.sun.ac.za/ctscanner/, accessed 14.06.2016.
[16] Mouton WBCJ. Initial study on the tensile creep of cracked steel fibre reinforced concrete. In: 8th RILEM international symposium on fiber reinforced concrete: challenges and opportunities. 2013. Online. Available: https://scholar.google.com/citations?view_op=view_citation&hl=th&user=9hznEYkAAAAJ&sortby=pubdate&citation_for_view=9hznEYkAAAAJ:qxL8FJ1GzNcC/, accessed: 19.02.16.
[17] Schrapp MJ, Herman GT. Data fusion in X-ray computed tomography using a superiorization approach. Rev Sci Instrum 2014;85(5):53701–11.
[18] Du Plessis A, Olawuyi BJ, Boshoff WP, Le Roux SG. Simple and fast porosity analysis of concrete using X-ray computed tomography. Mater Struct Constr 2016;49(1–2):553–62.
[19] Du Plessis A, Rossouw P. Investigation of porosity changes in cast Ti6Al4V rods after hot isostatic pressing. J Mater Eng Perform 2015;24:3137–41.